Encapsulation of mRNA in lipid nanoparticles by membrane micromixing

Carla Atallah, Bastien Piegay, Véronique Chiavazza, Catherine Charcosset

Encapsulation of mRNA in lipid nanoparticles by membrane micromixing

Carla ATALLAH[1] , Bastien PIEGAY[2], Véronique CHIAVAZZA[2], Catherine CHARCOSSET[1]*

(1) Univ Lyon, Université Claude Bernard Lyon 1, CNRS, LAGEPP UMR 5007, 43 Boulevard du 11 Novembre 1918, F-69100, Villeurbanne, France

(2) Sanofi, mRNA Center of Excellence, 1541 avenue Marcel Mérieux 69280 Marcy l'Etoile France

*Corresponding author: Tel.: +33 4 72 43 18 34

Email address: catherine.charcosset@univ-lyon1.fr (Catherine Charcosset)

Current affiliation of Carla Atallah , Sanofi, mRNA Center of Excellence, 1541 avenue Marcel Mérieux 69280 Marcy l'Etoile France

Abstract

Messenger RNA encapsulated in lipid nanoparticles (mRNA-LNPs) are successfully used worldwide for vaccination against COVID-19. mRNA-LNPs are manufactured by mixing an ethanolic phase (containing an ionizable lipid, a phospholipid, a PEGylated lipid and cholesterol) and an aqueous phase (citrate buffer at pH 4.5 containing mRNA). The characteristics of the mRNA-LNPs obtained (size, internal structure, mRNA functional delivery in vivo, etc) depend on several parameters and among them are the mixing conditions of the ethanolic and aqueous phases. While the impact of these parameters is well-recognized for small scale preparations (some microliters), their effect at a larger scale is less well-known. The purpose of this study is to investigate the production of some hundreds of millilitres of mRNA-LNP suspension using a ceramic membrane (SPG Technology) as a new mixing device. Summarily, in this technique, the ethanolic phase permeates through the membrane pores and mixes with the aqueous phase flowing in a small annular pipe between the tubular membrane and an inside rod. First, empty LNPs were prepared to determine the effect of membrane pore size, flow rate, and the ratio between the ethanolic and aqueous phase volumes. The experimental conditions tested did not change the characteristics of the LNPs obtained. Second, mRNA-LNPs were prepared and the suspensions obtained were then submitted to buffer exchange/concentration/ sterile filtration dialysis. The resulting mRNA-LNPs had a particle size of 103 ± 5 nm, a polydispersity index of 0.15 ±0.005, and encapsulation efficiency of 96 ± 0.0%. mRNA-LNPs with similar characteristics were obtained using ethanol ratios of 1/4 (20 % ethanol in the final preparation) and 1/6 (14% ethanol). Overall, membrane micromixing using a ceramic membrane was shown to be a suitable technology for the preparation of mRNA-LNP suspensions.

Keywords: Lipid nanoparticle, mRNA, membrane micromixing, membrane micromixer, encapsulation, nanoprecipitation.

1. Introduction

Messenger RNA encapsulated in lipid nanoparticles (mRNA-LNPs) are successfully used worldwide for vaccination against COVID-19 (Tsakiri et al. 2021, Schoenmaker et al. 2021, Park et al. 2021, Kim et al. 2021). They consist in the most successful non-viral mRNA delivery technology. mRNA is encapsulated in the LNPs core, protecting it from degradation by water and RNAses. The encapsulation ability is facilitated by the composition of the LNPs, i.e. an ionizable lipid, a phospholipid, a PEGylated lipid, and cholesterol. The ionizable lipid is considered the most critical factor, as its structure enables endosomal escape which is considered to be a rate limiting step for mRNA intracellular delivery. mRNA-LNPs are obtained by the ethanol injection method in which the ethanolic phase (containing lipids and cholesterol) and the aqueous phase (buffer containing mRNA) are mixed in a tight space. mRNA-LNPs are instantaneously formed by nanoprecipitation (also called antisolvent precipitation or phase separation) occurring when lipid molecules are supersaturated. Nanoprecipitation mainly involves nucleation and growth of mRNA and lipids nuclei and both processed define the final properties of the mRNA-LNPs (size, internal structure, mRNA functional delivery in vivo, etc) (Schoenmaker et al. 2021, Kim et al. 2021).

mRNA-LNPs are typically composed of an ionizable lipid, a phospholipid, a PEGylated lipid, and cholesterol, each compound having a specific role within the mRNA-LNPs structure (Tsakiri et al. 2021, Schoenmaker et al. 2021, Park et al. 2021, Kim et al. 2021). mRNA-LNPs are usually described as having a spherical, homogeneous, and dense structure. The PEGylated lipid is mainly located on the particles' surface, while mRNA is bound to the cationic or ionizable lipid inside the nanoparticle core which also contains water (Arteta et al. 2018, Viger-Gravel et al. 2018). LNPs are usually produced by microfluidics-mixing techniques as the NanoAssemblr from Precision NanoSystems, to study LNPs morphology, surface property and degradability, in vitro profiling and intracellular fate and in vivo application of LNP formulations (Cui et al. 2022). However, the microfluidic-mixing technology has usually a low-throughput preparation, which limits its application in the production of mRNA-LNPs at large scale.

At small scale (some microliters), mRNA-LNPs are prepared with a microfluidic device (e.g. Sabnis et al. 2018, Patel et al. 2019, Lou et al. 2020, Hassett et al. 2021). The ethanolic and aqueous phases are mixed in a tight microfluidic set-up at optimized mixing volumes, mixing speed, and total flow rate (Cui et al. 2021 and 2022, Hassett et al. 2021). The mRNA-LNPs final properties depend on several parameters, including the formulation (type of lipids, molar ratios of each compound, ratio between ethanolic and aqueous phase volumes, etc) and processing parameters (total flow rate, mixing duration and speed, hold time between mixing and buffer exchange, etc). Studies have reported the influence of the ethanolic and aqueous phases mixing on the mRNA-LNPs characteristics. Hassett et al. (2021) were able to decrease the mRNA-LNPs size by increasing the total flow rate during mixing. Indeed, increasing the total flow rate during formulation improves the mixing of the two phases and decreases the time allocated for particle formation, thus resulting in smaller particles. Cui et al. (2021 and 2022) prepared mRNA-LNPs in a new automated system based on a classical liquid handling device with 96 well-plates (60 μL) commonly used in labs. The mRNA-LNPs obtained were larger, presented higher mRNA loading per particle, and showed a 4.5-fold improvement in the in vivo delivery of functional mRNA compared to mRNA-LNPs of the same formulation obtained using a classical microfluidic system. Large LNPs tend to have a higher mRNA loading per particle, more hydrophobic surface, and more hemolytic and beneficial cellular uptake pathways (Cui et al. 2022). This difference in the particle characteristics was attributed to the precise mixing of the automated system.

Mixing of the ethanolic and aqueous phases is also a key step in the process design for the scaling up of mRNA-LNPs production. However, and to the best of our knowledge, relations between mixing

systems, their parameters, and the resulting mRNA-LNPs characteristics has yet to be discussed in the literature. Many mixing geometries can be used to perform solvent precipitation processes, such as T-junction mixers, microfluidic hydrodynamic focusing, and two-inlet or four-inlet vortex mixers (Saad and Prud'homme 2016, Evers et al. 2018, Liu et al. 2019, Xu et al. 2022). Other micromixing approaches have been proposed, such as the "crossflow" system developed in the 2000's by Wagner (Wagner et al. 2002). Made of two stainless steel tubes welded together to form a cross and connected with a 250 µm injection hole, this crossflow system allows to control mixing between the ethanolic and aqueous phases to obtain nanoparticles with the required properties. By controlling solute nucleation and growth rates in solvent precipitation processes, high loading efficiencies, loading contents, control of particle size, and flexibility in incorporating multiple actives are obtained (Saad and Prud'homme 2016).

Membrane micromixing is yet another mixing technique to produce nanoparticles by nanoprecipitation (Charcosset et al. 2007, Piacentini et al. 2022). Various membranes can be used such as polymeric and ceramic, with various geometries such as hollow fibers and tubes. This approach allowed producing several nanocolloids, including polymer nanocapsules (Limayem et al. 2006), solid lipid nanoparticles (D'Oria et al. 2009), chitosan nanoparticles (Hassani et al. 2015) and liposomes (Jaffar et al. 2011). In this method, the organic phase (in which the material to precipitate is dissolved) is injected through the pores of a microporous membrane; the aqueous phase circulates on the other side of the membrane (Figure 1). Micromixing between the two phases takes place at the exit of the membrane pores to produce a suspension of nanoparticles, whose size can be changed by changing the formulation and process conditions (Charcosset et al. 2007, Piacentini et al. 2022). The system gives high production rates and can be scaled up by increasing the membrane surface. Like the crossflow system, membrane micromixing allows for a continuous production of nanoparticles.

The aim of this study was to investigate the preparation of mRNA-LNPs by membrane micromixing for volumes of some hundreds of millilitres. A model cationic lipid (1,2-dioleoyl-3-trimethylammonium-propane chloride (DOTAP-Cl)) was used and the ceramic membrane had a tubular shape (SPG Technology, Japan). The potential of the membrane micromixing method to prepare mRNA-LNPs was evaluated, in particular the influence of the total flow rate and of the ethanolic and aqueous phases volume ratio ($V_{eth}/V_{aq)}$ on the characteristics of the mRNA-LNPs obtained.

The study included three main steps. First, empty LNPs were prepared by membrane micromixing at different operating conditions (ie, membrane pore size, total flow rate, V_{eth}/V_{aq} of 1/4 and 1/6) to choose the optimal operating conditions for the preparation of mRNA-LNPs. Next, mRNA-LNPs were prepared for V_{eth}/V_{aq} of 1/4 and 1/6 and the obtained suspensions were processed through dialysis, centrifugation, and sterile filtration for evaluation and characterization of LNPs and mRNA-LNPs. Last, the size and the polydispersity index (pdI) of all LNPs were measured. mRNA-LNPs were characterized by the encapsulation efficiency (EE), cryo-Transmission Electron Microscopy (cryo-TEM) observations, and stability measurements. As the final part of our assessment of this approach, we calculated mRNA yields.

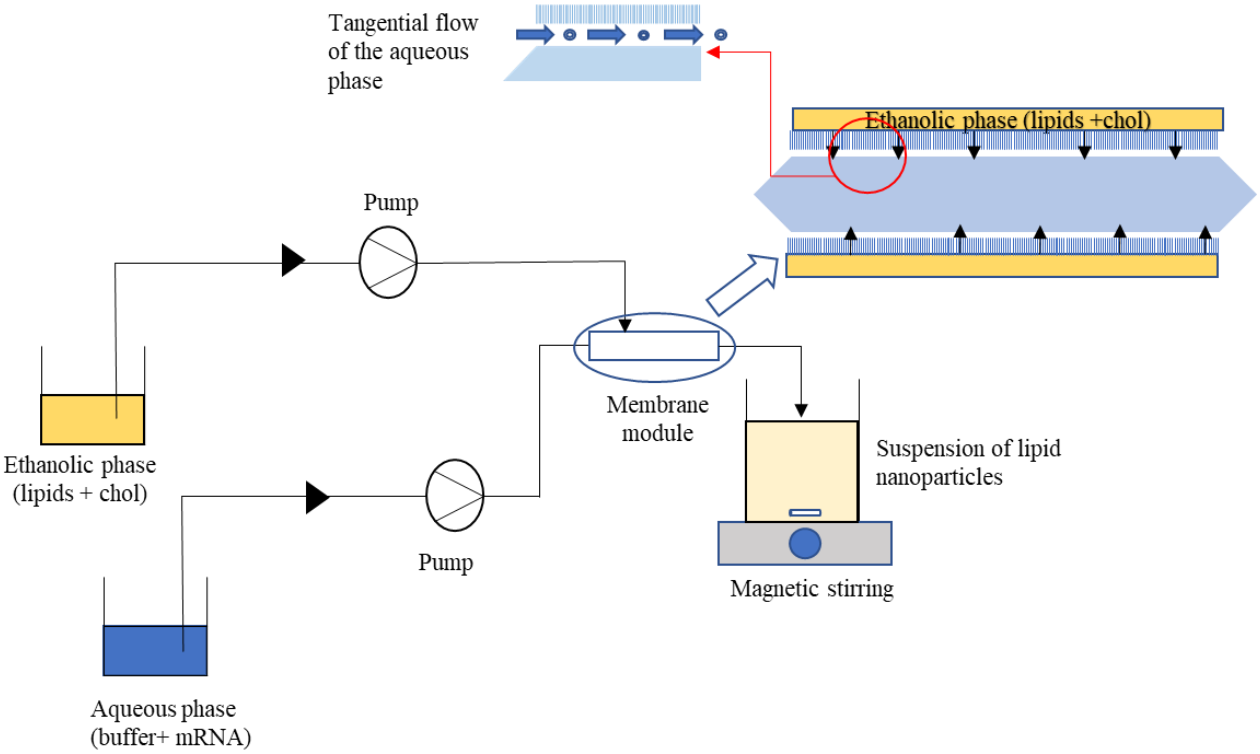

Figure 1: Preparation of LNPs by membrane micromixing

2. Materials and Methods

2.1 Materials

The following phospholipids were purchased from Lipoid (France): the cationic lipid 1,2-dioleoyl-3-trimethylammonium-propane chloride (DOTAP-Cl), the neutral lipid 1,2-dioleoyl-sn-glycero-3-phosphoethanolamine (DOPE) and the PEGylated lipid N-(carbonyl-methoxypolyethylenglycol-2000)-1,2-distearoyl-*sn*-glycero-3-phosphoethanolamine, sodium salt (MPEG-2000-DSPE; henceforth referred to as PEG2000-Lipid). Other chemicals used were cholesterol (Sigma Aldrich, France), 99% ethanol (Carlo Erba Reagents, France), citric acid monohydrate and trisodium citrate dehydrate (Fisher Chemicals, France), phosphate buffered saline (PBS) (Sigma Aldrich, France), and trehalose dihydrate (Pfanstiehl, Switzerland). mRNA was provided by Sanofi mRNA Center of Excellence (Marcy l'Etoile, France).

Consumables included Amicon Ultra-15 tubes (100 kD) (Merck Millipore, France) for centrifugation, Slide-A-Lyzer dialysis cassettes (10 kD, volume 3-12 mL) (Thermofisher, France) for dialysis and 0.2 µm polyethersulfone syringe filters, diameter 13 mm (Pall, France) for sterile filtration.

Ultrapure water was obtained using a Synergy unit system (Merck Millipore, France). RNase-free water (Dutscher, France) was used for mRNA-LNPs preparation.

2.2 Formulations

The formulation used was DOTAP:DOPE:Cholesterol:PEG2000-Lipid (40:30:28.5:1.5 molar ratio). The ethanolic phase was prepared by dissolving the lipids and cholesterol in ethanol. The dissolution was carried out using magnetic agitation. For the V_{eth}/V_{aq} ratio of 1/4 and of 1/6 the lipid concentration in ethanol was 10 mg/mL and 14 mg/mL, respectively.

For empty LNP formulations, the aqueous phase was PBS. For mRNA-LNP preparations, the aqueous phase was citrate buffer pH 4.5 prepared with RNase-free water. The mRNA solution provided by Sanofi had a concentration of 1 mg/mL. The aqueous phase was prepared to have a final concentration of mRNA after nanoprecipitation equal to 0.08 mg/mL.

2.3 Membrane micromixing

2.3.1 SPG module and membrane

SPG membranes were supplied by SPG Technology (Japan) (Figure 2). These membranes are made from Shirasu (volcanic ash from a region of Japan) and are composed mainly of SiO_2 and Al_2O_2. They have a regular and interconnected porous structure (Vladisavljević et al. 2005).

The SPG membranes used in this study were tubular in form with a length of 125 mm, an internal diameter of 8.3 mm, and a thickness of 0.75 mm. The membrane was positioned inside a stainless-steel module (SPG Technology). To maintain a good seal, two O-rings were placed at the ends of the membrane, which reduced the effective length to approximately 100 mm. Hydrophilic membranes of three different pore sizes (2, 5, and 10 μm) were tested. The membrane with pore size of 10 μm was used in all experiments, except for the influence of membrane pore size where membranes with 2 and 5 μm were tested.

A polytetrafluoroethylene (PTFE) rod (6.3 mm diameter) was placed inside the tubular membrane. The addition of the rod allows to create an annular pipe of 1 mm where the mixing between the two phases takes place (Melich et al. 2019).

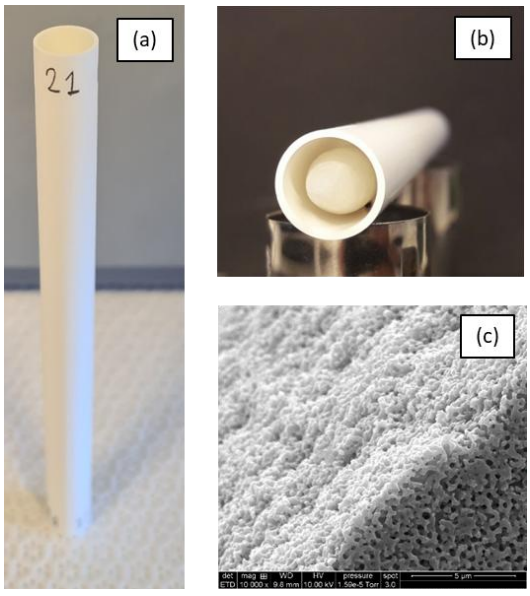

Figure 2: Images of (a) the SPG tubular membrane, (b) the PTFE rod inside the membrane and (c) a scanning electron microscopy (SEM) image of the membrane surface.

2.3.2 Experimental set-up

Figure 1 shows the experimental setup used for the preparations of LNPs. The setup included two Quattroflow 150 S pumps for the circulation of the aqueous and ethanolic phases. Mixing between

the ethanolic and aqueous phases occurred in a very narrow space between the inner surface of the tubular membrane and the rod placed inside. The suspension of LNPs formed was recovered at the outlet of the membrane device. The experiments were carried out at ambient temperature (21 ± 1°C).

2.3.3 Operating protocol

The ethanolic and aqueous phases were prepared in beakers that were installed on the experimental set-up; the pumps were started and the tubings filled with their respective phase. Typically, the experiment was performed for 30 s at a total flow rate of 500 mL/min. The mixed preparation of LNPs was collected at the outlet of the membrane module. The first milliliters of the preparation were discarded and the remainder was taken for storage and characterization. Before storage, the mixed preparation was stirred for 15 min. At the end of each run, the experimental set-up was washed by circulating water. Finally, the membrane was removed from the module, put in a glass tube containing 99% ethanol, and placed in an ultrasound bath for 2 h. The tube was then emptied, the ethanol replaced by ultrapure water, and the tube placed again in the ultrasonic bath for 15 min. This operation was repeated once.

2.3.4 Operating parameters for the preparation of empty LNPs

The optimization of the process was carried out during the preparation of blank LNPs. Various operating parameters were tested: the membrane pore size, total flow rate (Q_{total}), and V_{eth}/V_{aq} ratio. Lipid concentration in the ethanolic phase was either 10 or 14 mg/mL, depending on the V_{eth}/V_{aq} ratio. Three total flow rates were tested: 500, 750, and 1000 mL/min. The aqueous and ethanolic phases flow rates were selected to ensure continuous and homogeneous mixing conditions over the entire run duration (ie, 30 s). The flow rates and volumes are given in Table 1. The preparations were made for a volume ratio of 1/4, i.e. 20% ethanol. A ratio of 1/6 was also tested, allowing the amount of ethanol to be reduced to 14%.

Table 1: Volumes and flow rates of the aqueous and ethanolic phases at different total flow rates (with the indices eth: ethanol, aq : aqueous)

V_{eth}/V_{aq} ratio	Q_{total} (mL/min)	Q_{aq} (mL/min)	V_{aq} (mL)	Q_{eth} (mL/min)	V_{eth} (mL)	T (s)	V_{final} (mL)
1/4	500	400	200	100	50	30	250
	750	600	300	150	75	30	375
	1000	800	400	200	100	30	500
1/6	500	428.6	214.3	71.4	35.7	30	250

2.3.5 Operating parameters for the preparation of mRNA-LNPs

The protocol carried out for the preparation of mRNA-LNPs was identical to the one for empty LNPs. The experiments were done at ambient temperature (21 ± 1 ° C). The mRNA-LNPs were prepared with the SPG membrane of pore size 10 µm. V_{eth}/V_{aq} ratios of 1/4 and 1/6 were tested. The total flow rate was 500 mL/min. All experiments were performed in triplicate.

2.4. Post-processing of mRNA-LNPs

The suspensions of mRNA-LNPs obtained by nanoprecipitation were treated by dialysis, centrifugation, and sterile filtration. Dialysis is aimed at changing the ethanolic solution by RNase-free water, centrifugation using membranes (100 kD MWCO) to concentrate the nanoparticles to the required mRNA concentration, and sterile filtration with 0.2 µm pore size membrane sterilizes the final product.

The formulations were dialysed using Slide-A-Lyzer dialysis cassette (10 kD) under magnetic agitation, first with 80/20 % RNase-free water/ethanol solution, then with RNase-free water alone. The suspensions were then concentrated in a trehalose 10% (w/v) using centrifugation by Amicon Ultra-15 tubes (100 kD). Post-processing, the lipid concentration was 24 mg/mL and the RNA concentration 0.96 mg/mL. Last, the formulations were filtrated using 0.2 µm filters.

2.5 Characterization of LNPs

LNPs obtained were characterized by their intensity weighted mean hydrodynamic diameter (Z-average) and pdI. These parameters were measured on a Zetasizer Nanoseries (Malvern). The size and pdI were obtained by the Dynamic Light Scattering (DLS) method. All measurements were carried out at 25 °C after 2 min of equilibration and were performed in triplicate. Data were expressed as the mean values ± SD. Free and total mRNA concentrations were measured by RiboGreen assay. Data were expressed as the mean values ± SD of independent triplicate experiments. The EE of mRNA was calculated as the encapsulated concentration (total measured concentration minus free concentration divided by the total measured concentration). The yield of the process was evaluated as the measured total concentration divided by the theoretical total concentration. The yield gave an indication of the process efficiency.

The EE and yield were calculated according to equation 1 and 2. These two parameters were measured after nanoprecipitation and after post-treatment.

$$\text{EE (\%)} = \frac{[mRNA]_{encapsulated}}{[mRNA]_{total\ measured}} \quad (1)$$

$$\text{with } [mRNA]_{encapsulated} = [mRNA]_{total\ measured} - [mRNA]_{free}$$

$$\text{Yield (\%)} = \frac{[mRNA]_{\ total\ measured}}{[mRNA]_{total\ theoretical}} \quad (2)$$

where $[mRNA]_{encapsulated}$ is the encapsulated concentration, $[mRNA]_{total\ measured}$ is the total measured concentration, $[mRNA]_{free}$is the free concentration, and $[mRNA]_{total\ theoretical}$is the theoretical total concentration.

Cryo-TEM observations were made at the Centre Technologique des Microstructures, Université Claude Bernard Lyon 1 (Villeurbanne, France). The samples were deposited on 200-mesh perforated carbon films (Lacey) then frozen in liquid ethane using a Vitrobot (ThermoFisher Scientific). The samples were mounted on a Gatan 626 sample holder precooled with liquid nitrogen, then observed under a microscope (Phillips CM120) using a Gatan Orius 200 camera. The observations were carried out in low dose mode at a voltage 120 kV acceleration, spot 5.

The characteristics of the LNPs (size, pdI and EE) and process yield were measured after 2 months of storage for the preparations made at V_{eth}/V_{aq} ratio of 1/4. Storage was carried out at 4°C.

3.Results and discussion

3.1 Preparation of blank LNPs

Blank LNPs were prepared through a range of operating conditions: membrane pore size, total flow rate, and ratio V_{eth}/V_{aq}. The characteristics of the LNPs obtained are provided in Figure 3 as a histogram with standard deviations.

3.1.1 Influence of membrane pore size

Membranes with different pore size (2, 5, and 10 μm) were tested while keeping the same total flow rate of 500 mL/min and V_{eth}/V_{aq} ratio of 1/4. LNPs size ranged between 115 and 130 nm and the pdI between 0.20 and 0.21, indicating a rather narrow size distribution. The SPG membrane with pore size 10 μm was selected for the following experiments as it gave the smallest size (115 ± 10 nm), compared to the 2 μm (130 ± 10 nm) and 5 μm membranes (120 ± 10 nm). The NP size decreased slightly with the membrane pore size suggesting that the velocity field obtained using the membrane with larger pore favours small nanoparticle sizes.

3.1.2 Influence of total flow rate

Three total flow rates were tested, 500, 750, and 1000 mL/min, with the 10 μm pore size membrane at a V_{eth}/V_{aq} ratio of 1/4. An increase in total flow rate is interesting for the manufacturing process as it allows decreasing production time. LNPs with similar size were obtained for the three flow rates, between 115 and 120 nm and pdI between 0.19 and 0.22. Although a 1000 mL/min flow rate allowed generating LNPs with suitable characteristics, the lowest total flow rate (500 mL/min) was used to further characterize the membrane micromixing approach as it allowed sparing raw materials.

3.1.3 Influence of V_{eth}/V_{aq} ratio

The reduction of ethanol consumption in the manufacturing process allows for decreased production cost and facilitates the management of solvent. A V_{eth}/V_{aq} ratio of 1/6 was tested (14% ethanol in the final preparation) for comparison with the 1/4 ratio (20% ethanol). At V_{eth}/V_{aq} of 1/6, the initial lipid concentration in the ethanolic phase was higher than at 1/4 (14 mg/mL instead of 10 mg/mL), to keep the same final lipid concentration of 2 mg/mL. This adds an additional challenge for the consistent production of LNPs with a narrow size distribution as higher lipid concentrations tend to lead to the formation of larger particles and/or aggregates. This phenomenon is well known for preparation of polymeric nanoparticles by nanoprecipitation. As polymer concentration increases, its corresponding nucleation and growth rates increase faster than the polymer aggregation rate, providing additional time for particle growth before polymer stabilization, and resulting in larger particle size (Saad and Prud'homme 2016).

At V_{eth}/V_{aq} ratio of 1/6, the LNPs obtained had similar characteristics to those produced with a 1/4 ratio, with particle size of 120 ± 10 nm and pdI of 0.21 ± 0.02, versus 115 ± 10 nm and pdI 0.20 ± 0.02. This suggests that it is possible to prepare LNPs with a lower amount of ethanol using a membrane micromixer. Thus, mixing between the ethanolic and aqueous phases in the membrane micromixer creates suitable conditions to form nanometric LNPs even at higher lipid supersaturation.

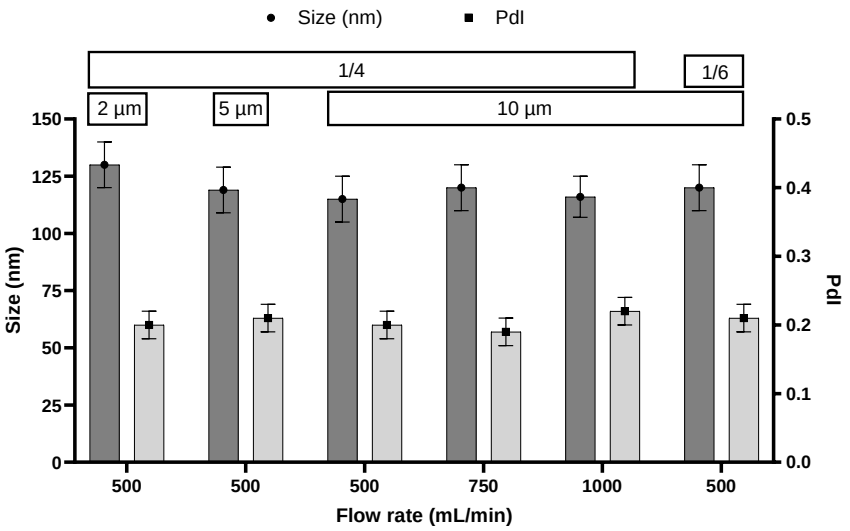

Figure 3: Characteristics of empty LNPs obtained by nanoprecipitation – Influence of operating parameters (membrane pores: 2, 5, and 10 µm; V_{eth}/V_{aq} ratios of 1/4 and 1/6; flow rates: 500, 750, and 1000 mL/min).

3.2 Preparation of mRNA-LNPs

mRNA-LNPs were prepared by nanoprecipitation and then submitted to dialysis, centrifugation and sterile filtration (post-treatment). Characteristics of the mRNA-LNPs obtained post-treatment steps are given as a histogram in Figure 4. Similarly, to the preparation of blank LNPs, the two different V_{eth}/V_{aq} ratios (1/4 and 1/6) were tested.

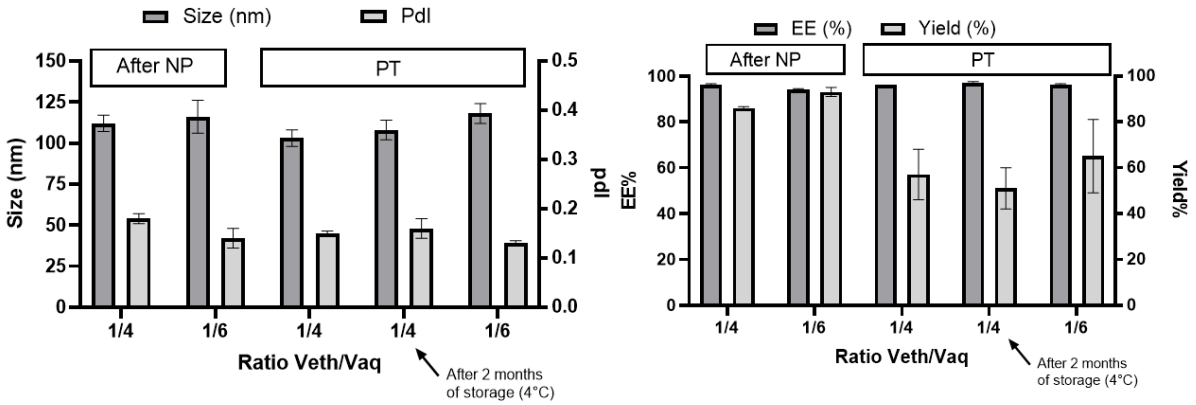

Figure 4: Characteristics of mRNA-LNPs obtained after nanoprecipitation and post-treatment – 10 µm SPG membrane and total flow rate 500 mL/min (after preparation and after 2 months of storage at 4°C) (NP: nanoprecipitation and PT: post-treatment)

3.2.1 V_{eth}/V_{aq} ratio of 1/4

The mRNA-LNPs obtained after nanoprecipitation had a size of 112 ± 5 nm and pdI of 0.18 ± 0.01. The size and pdI were slightly lower than the values obtained for blank LNPs. Arteta et al. (2018) observed an opposite effect with mRNA-LNPs being significantly larger than blank LNPs. In both cases, this confirm that mRNA contributes to the formation and structure of mRNA-LNPs. The involvement of mRNA in LNP constitution was confirmed by dynamic nuclear polarization NMR spectroscopy (Viger-Gravel et al. 2018).

The mean particle size (Z-average) and pdI of the mRNA-LNPs decreased slightly post-treatment, and were of 103 ± 5 nm and pdI of 0.15 ± 0.005, respectively. This is most likely the result of the post-treatment filtration (0.2 μm) as this step not only sterilized the preparation but also removed any large particles that may be present in the suspension. Figure 5 shows DLS graphs of mRNA-LNPs obtained after post-treatment. The measurements were done on three batches obtained during different manufacturing. The similarity of the three DLS curves confirms the reproducibility of the process.

A wide range of mRNA-LNPs' particle mean size and pdI values are reported in the literature as many factors affect the particles' characteristics. The anionic or ionizable lipid has a key role in obtaining mRNA-LNPs with a specific size and/or a narrow size distribution (Arteta et al. 2018, Patel et al. 2019). Other factors include the V_{eth}/V_{aq} ratio, the total flow rate, and the mixing device used (e.g. Hassett et al. 2021, Cui et al. 2021 and 2022). The elasticity of the nanoparticles may have also a role on the final nanoparticles properties (Guo et al. 2018, Hui et al. 2020). It is usually admitted that the pdI ought to be lower than 0.2, although the precise effect of pdI on mRNA functional delivery in vivo remains difficult to evaluate. Even the influence of the mRNA-LNPs particle size on mRNA delivery is subject to discussion. Hassett et al. (2021) found that an average particle size of 100 nm gave optimal antibody titers in mice, while all particles size in the range they tested (60-150 nm) yielded robust immune response in non-human primates. Cui et al. (2021, 2022) obtained large mRNA-LNPs (147 ± 9 nm) with a new automated device that produced a 4.5-fold improvement in mRNA functional delivery in vivo compared to mRNA-LNPs prepared with a classical microfluidic system (73 ± 5 nm). The authors explained this result by the higher loading rate of the largest mRNA-LNPs. The surface characteristic of the mRNA-LNPs is also a key parameter in determining transfection efficacy in the cell types tested (Arteta et al. 2018). Overall, it seems that surface composition and mRNA loading rate are critical features of the functional delivery of mRNA in vivo, and these two parameters depend on the mRNA-LNPs particle size.

The EEs were 95.6 ± 0.6 % and 96.0 ± 0.0 %, after nanoprecipitation and post-treatment, respectively (Figure 4). These values are similar to EEs reported in the literature, that are usually in the range of 90-99% (e.g. Hassett et al. 2021, Cui et al. 2021).

The yield in mRNA-LNPs may give an idea of the loss of mRNA during the process. The yields were 85.7 ± 0.6 % and 56.8 ± 11.5 % after nanoprecipitation and post-treatment, respectively. Thus, the post-treatment (dialysis and centrifugation) led to mRNA degradation. Meanwhile the EEs were unchanged after post-treatment. Schoenmaker et al. (2021) suggested that the hydrolysis of mRNA might be the main factor for mRNA instability, and that it could occur both for mRNA in solution and encapsulated mRNA as the lipid core also contains water. This could explain the decrease in yield after post-treatment while the EE was unchanged.

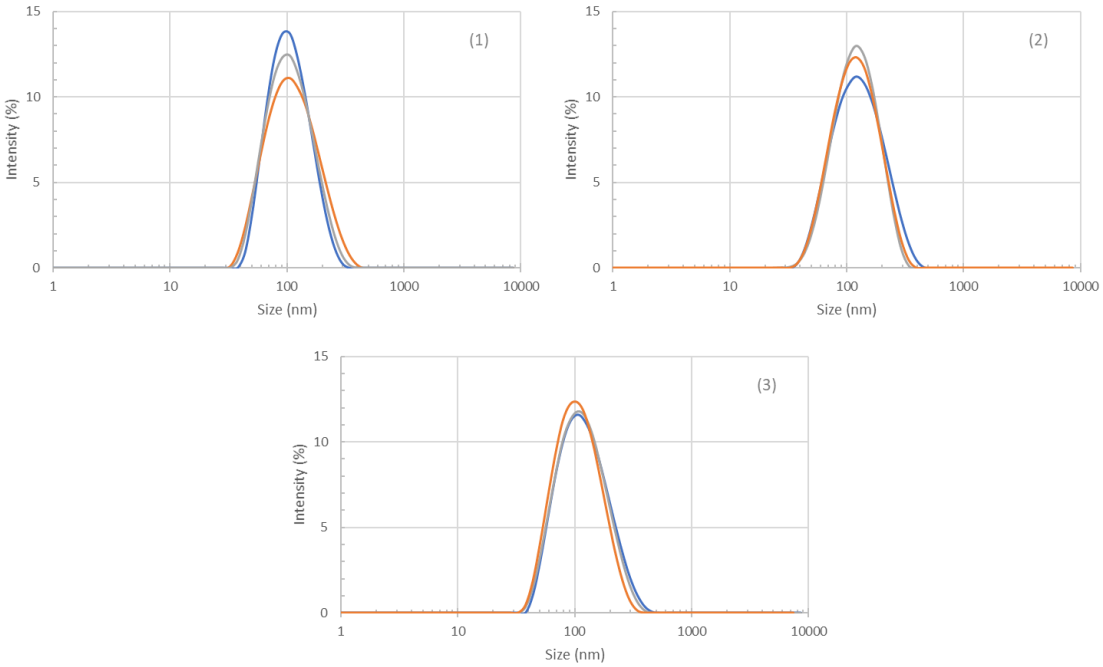

Figure 5: DLS measurement of mRNA-LNPs obtained after post-treatment (V_{eth}/V_{aq} ratio of 1/4). The DLS graphs 1 to 3 characterize independent preparations realized for the same experimental conditions (the 3 colours: blue, red, green correspond to 3 different DLS measurements).

To further characterized the mRNA-LNP particles obtained, the post-treatment suspensions were observed by cryo-TEM. The images showed spherical and dense structures (Figure 6a). The larger structures (surrounded by black lines) corresponded to the holes in the support used to deposit the sample. The cryo-TEM images showed that the size of the LNPs was less than 100 nm, smaller than what was observed by DLS (Figure 6b). This has been documented by others (Cui et al. 2021) and could be due to some of the differences between the two techniques. Among others, DLS measures the hydrodynamic radius from changes in the light scattering, which is very different to the actual size; the samples of DLS are solvated while cryo-TEM works on freeze-dried dry samples; also, DLS measures a larger number of particles (millions) compared to TEM (few hundreds) (Bhattacharjee 2016). This contributes to obtain usually larger LNPs size by DLS than by cryo-TEM as observed by Cui et al. (2021). It is noteworthy that the micrographs show very few “blebs” compared to what was observed by others (e.g. Brader et al. 2021). Indeed, the mRNA-LNP structure may involve solvent pockets, called “blebs”. Blebs are referred as structural defects and may be empty or mRNA loaded (Brader et al. 2021).

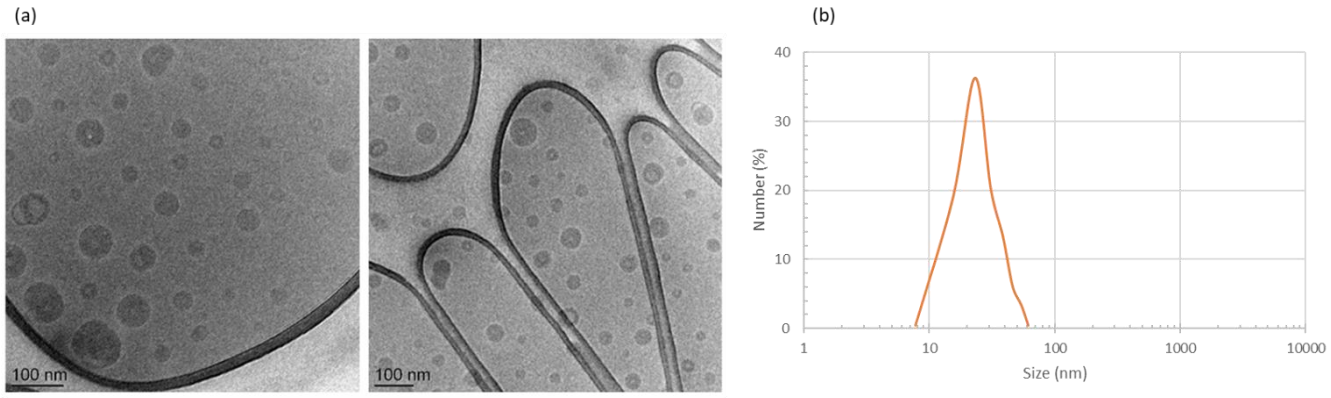

Figure 6: (a) Cryo-TEM images of mRNA-loaded LNPs (V_{eth}/V_{aq} ratio of 1/4), (b) size distribution obtained from cryo-TEM images (measured on 230 LNPs)

3.2.2 V_{eth}/V_{aq} ratio of 1/6

After nanoprecipitation, the LNPs obtained had a size of 116 ± 10 nm and a pdI of 0.14 ± 0.02. The EE was 93.6 ± 0.5 % and the yield 92.5 ± 2.1 %. Similar to what was observed with the 1/4 ratio, post-processing did not change the LNPs size (118 ± 6 nm) and pdI (0.13 ± 0.005). The EE was 95.6 ± 0.57 % and the yield decreased to 64.6 ± 16.5 % after post-treatment (decrease of 30%). Thus, the mRNA-LNPs had similar characteristics at V_{eth}/V_{aq} ratio of 1/4 and 1/6.

3.2.3. Stability study

The development of a mRNA vaccine to market requires that the candidate has a satisfactory shelf-life, preferably at refrigerator temperatures (2-8°C), to make worldwide distribution possible (Schoenmaker et al. 2021). To study stability, the mRNA-LNPs prepared by membrane micromixing were stored at 4°C for 2 months and then characterized for their size, pdI, EE, and yield after of storage (Figure 4). After 2 months, the mRNA- LNPs characteristics were almost unchanged, with the size of 108 ± 6 nm, pdI of 0.16 ± 0.02 and the EE 96.6 ± 0.6 %; the yield was 51.1 ± 9.5 %. Compared to initial values, the size, pdI, EE% and yield remained stable.

4. Conclusion

In this study, we prepared mRNA-LNPs using nanoprecipitation with a membrane micromixing device. The membrane was a SPG ceramic membrane with a tubular shape. DOTAP was used as a model cationic lipid. Blank LNPs were first prepared with size between 120 - 130 nm and pdI between 0.16 and 0.22. Although most of the mRNA-LNPs characterization was performed on particles obtained at a flow rate of 500 mL/min, this study showed that blank LNPs could well be prepared at a higher flow rate of 1000 mL/min.

The mRNA-LNPs were then prepared by membrane micromixing at V_{eth}/V_{aq} ratio of 1/4. Post-treatment, the mRNA-LNPs an intensity weighted mean hydrodynamic diameter measured by DLS of 103 ± 5 nm and were homogeneous (pdI = 0.15 ± 0.005) which was confirmed by cryo-TEM. The EEs were high (96 ± 0.0 %), suggesting that the cationic lipid DOTAP is effective in binding the negatively charged mRNA molecules. A Veth/Vaq ratio of 1/6 (14% ethanol) made it possible to prepare LNPs with characteristics similar to those obtained with a V_{eth}/V_{aq} ratio of 1/4 (20 % ethanol). Also, the processing by dialysis, centrifugation, and sterile filtration was shown to decrease the loading rate

while keeping the same encapsulation efficiency, suggesting mRNA degradation of both free and encapsulated mRNA.

Overall, membrane micromixing was shown to be a suitable technology for the preparation of mRNA-LNPs. Micromixing conditions created in the annular pipe between the inner microporous surface of the membrane and the insertion rod makes possible to obtain mRNA-LNPs with the desired characteristics. In this study, several hundreds of milliliters were prepared in 30 s, further scale-up will require the production of several liters of mRNA-LNP suspensions.

Acknowledgements

The authors would like to thank Sanofi for financial support, for providing the mRNA, and for the mRNA concentration measurements. Editorial assistance was provided by Jean-Sébastien Bolduc from Sanofi.

Funding:

This work was funded by Sanofi.

Disclosure of interest:

Carla Atallah, Bastien Piegay et Véronique Chiavazza are Sanofi employees and may hold shares and/or stock options in the company. C. Charcosset (Université Claude Bernard Lyon 1, CNRS) declares no competing financial interest.

Credit author statement :

Carla ATALLAH : Methodology, Investigation, Formal analysis, Visualization, Validation, Writing - Review & Editing; **Bastien PIEGAY :** Methodology, Investigation, Resources, Writing - Review & Editing; **Véronique CHIAVAZZA :** Conceptualization, Funding acquisition, Supervision, Writing - Review & Editing; **Catherine CHARCOSSET :** Conceptualization, Funding acquisition, Project administration, Supervision, Resources, Writing - Original Draft, Writing - Review & Editing

Bibliography

Arteta M.Y., Kjellman T., Bartesaghi S., Wallin S., Wu X., Kvist A.J., Dabkowska A., Székely N., Radulescu A., Bergenholtz J., Lindfors L. Successful reprogramming of cellular protein production through mRNA delivered by functionalized lipid nanoparticles. PNAS, 115 (2018) E3351–E3360

Bhattacharjee S., DLS and zeta potential – What they are and what they are not? Journal of Controlled Release, 235 (2016) 337–351.

Brader M.L., Williams S.J., Banks J.M., Hui W.H., Zhou Z.H., Jin L. Encapsulation state of messenger RNA inside lipid nanoparticles. Biophysical Journal, 120 (2021) 2766–2770.

Charcosset C., Bernard S., Fiaty K., Bechelany M., Cornu D. Membrane techniques for the preparation of nanomaterials: Nanotubes, Nanowires and Nanoparticles – A review. *In* Dynamic Biochemistry, Process Biotechnology and Molecular Biology. Global Science Books 1 (2007) 15-23

Cui L., Hunter M.R., Sonzini S., Pereira S., Romanelli S.M., Liu K., Li W., Liang L., Yang B., Mahmoudi N., Desai A.S. Mechanistic studies of an automated lipid nanoparticle reveal critical pharmaceutical properties associated with enhanced mRNA functional delivery in vitro and in vivo. Small (2021) 2105832.

Cui L., Pereira S., Sonzini S., van Pelt S., Romanelli S.M., Liang L., Ulkoski D., Krishnamurthy V.R., Brannigan E., Brankine C., Desai A.S. Development of a high-throughput platform for screening lipid nanoparticles for mRNA delivery. Nanoscale 14 (2022) 1480–1491.

D'Oria C., Charcosset C., Barresi A., Fessi H., Preparation of solid lipid particles by membrane emulsification: influence of process parameters. Colloids and Surfaces A, 338 (2009) 114–118.

Evers M.J.W., Kulkarni J.A., van der Meel R., Cullis P.R., Vader P., Schiffelers R.M. State-of-the-art design and rapid-mixing production techniques of lipid nanoparticles for nucleic acid delivery. Small Methods, 2 (2018) 1700375.

Guo P., Liu D, Subramanyam K., Wang B., Yang J., Huang J., Auguste D.T., Moses M.A., Nanoparticle elasticity directs tumor uptake, Nature Communications (2018) 9:130

Hassani S., Laouini A., Fessi H., Charcosset C., Preparation of chitosan–TPP nanoparticles using microengineered membranes – Effect of parameters and encapsulation of tacrine. Colloids and Surfaces A, 482 (2015) 34-43.

Hassett K.J., Higgins J., Woods A., Levy B., Xia Y., Hsiao C.J., Acosta E., Almarsson O., Moore M.J., Brito L.A., Impact of lipid nanoparticle size on mRNA vaccine immunogenicity. Journal of Controlled Release, 335 (2021) 237-246.

Hui Y., Yi X., Wibowo D., Yang G., Middelberg A.P.J., Gao H., Zhao C.-X., Nanoparticle elasticity regulates phagocytosis and cancer cell uptake, Science Advances, 6 (2020) eaaz4316

Jaafar-Maalej C., Charcosset C., Fessi H. A new method for liposome preparation using a membrane contactor. Journal of Liposome Research, 21 (2011) 213–220.

Kim J., Eygeris Y., Gupta M., Sahay G. Self-assembled mRNA vaccines. Advanced Drug Delivery Reviews, 170 (2021) 83–112.

Limayem I., Charcosset C., Sfar S., Fessi H., Preparation and characterization of spironolactone-loaded nanocapsules for paediatric use. International Journal of Pharmaceutics, 325 (2006) 124–131.

Liu Y., Yang G., Zou D., Hui Y., Nigam K., Middelberg A.P.J., Zhao C.X., Formulation of nanoparticles using mixing-induced nanoprecipitation for drug delivery, Industrial and Engineering Chemistry Research 59 (2020) 4134-4149

Lou G., Anderluzzi G., Schmidt S.T., Woods S., Gallorini S., Brazzoli M., Giusti F., Ferlenghi I., Johnson R.N., Roberts C.W., O'Hagan D.T., Baudner B.C., Perrie Y. Delivery of self-amplifying mRNA vaccines by cationic lipid nanoparticles: The impact of cationic lipid selection. Journal of Controlled Release, 325 (2020) 370-379.

Melich R., Valour J.-P., Urbaniak S., Padilla F., Charcosset C. Preparation and characterization of perfluorocarbon microbubbles using Shirasu Porous Glass (SPG) membranes. Colloids and Surfaces A, 560 (2019) 233-243.

Park K.S., Sun X., Aikins M.E., Moon J.J. Non-viral COVID-19 vaccine delivery systems. Advanced Drug Delivery Reviews, 169 (2021) 137–151.

Patel S., Ryals R.C., Weller K.K., Pennesi M.E., Sahay G. Lipid nanoparticles for delivery of messenger RNA to the back of the eye. Journal of Control Release, 303 (2019) 91-100.

Piacentini E., Russo B., Bazzarelli F., Giorno L. Membrane nanoprecipitation: From basics to technology development. Journal of Membrane Science 654 (2022) 120564.

Saad W.S., Prud'homme R.K., Principles of nanoparticle formation by flash nanoprecipitation. nanotoday 11 (2016) 212-227.

Sabnis S., Kumarasinghe E.S., Salerno T., Mihai C., Ketova T., Senn J.J., Lynn A., Bulychev A., McFadyen I., Chan J., Almarsson Ö., Stanton M. G., Benenato K. E. A novel amino lipid series for mRNA delivery: Improved endosomal escape and sustained pharmacology and safety in non-human primates. Molecular Therapy, 26 (2018) 1509–1519.

Schoenmaker L., Witzigmann D., Kulkarni J.A., Verbeke R., Kersten G., Jiskoot W. , Crommelin D.J.A. mRNA-lipid nanoparticle COVID-19 vaccines: Structure and stability. International Journal of Pharmaceutics, 601 (2021) 120586.

Tsakiri M., Naziris N., Demetzos C. Innovative vaccine platforms against infectious diseases: Under the scope of the COVID-19 pandemic. International Journal of Pharmaceutics, 610 (2021) 121212.

Vladisavljević G.T., Shimizu M., Nakashima T., Permeability of hydrophilic and hydrophobic Shirasu-porous-glass (SPG) membranes to pure liquids and its microstructure. Journal of Membrane Science, 250 (2005) 69−77.

Viger-Gravel J., Schantz A., Pinon A.C., Rossini A.J., Schantz S., Emsley L. Structure of lipid nanoparticles containing siRNA or mRNA by dynamic nuclear polarization-enhanced NMR spectroscopy. Journal of Physical Chemistry B 122 (2018) 2073−2081.

Xu L., Wang X., Liu Y., Yang G., Falconer R.J., Zhao C.X., Lipid nanoparticles for drug delivery, Advanced NanoBiomed Research, 2 (2022) 2100109

Wagner A., Vorauer-Uhl K., Katinger H. Liposomes produced in a pilot scale: Production, purification and efficiency aspects. European Journal of Pharmaceutics and Biopharmaceutics, 54 (2002) 213–219.